Mon. Not. R. Astron. Soc. **000**, 1–6 (2005) Printed 5 February 2008 (MN LATEX style file v2.2)

# A multiwavelength investigation of the temperature of the cold neutral medium

Nirupam Roy[1] ⋆, Jayaram N. Chengalur[1⋆] and Raghunathan Srianand[2⋆]
[1]*NCRA-TIFR, Post Bag 3, Ganeshkhind, Pune 411 007, India*
[2]*IUCAA, Post Bag 4, Ganeshkhind, Pune 411007, India*



Accepted 2005 October 10. Received 2005 October 5; in original form 2005 May 19

**ABSTRACT**

We present measurements of the H I spin temperatures ($T_s$) of the Cold Neutral Medium (CNM) towards radio sources that are closely aligned with stars for which published $H_2$ ortho-para temperatures ($T_{01}$) are available from UV observations. Our sample consists of 18 radio sources close to 16 nearby stars. The transverse separation of the lines of sight of corresponding the UV and radio observations varies from 0.1 to 12.0 pc at the distance of the star. The ultraviolet (UV) measurements do not have velocity information, so we use the velocities of low ionization species (e.g Na I/ K I/ C I) observed towards these same stars to make a plausible identification of the CNM corresponding to the $H_2$ absorption. We then find that $T_{01}$ and $T_s$ match within observational uncertainties for lines-of-sight with $H_2$ column density above $10^{15.8}$ cm$^{-2}$, but deviate from each other below this threshold. This is consistent with the expectation that in the CNM $T_s$ tracks the kinetic temperature due to collisions and that $T_{01}$ is driven towards the kinetic temperature by proton exchange reactions.

**Key words:** ISM: atoms – ISM: molecules – radio lines: ISM – ultraviolet: ISM.

## 1 INTRODUCTION

Physical conditions in the interstellar medium (ISM) have traditionally been studied using spectral lines from a variety of tracers including the 21 cm line and recombination lines of hydrogen in the radio regime, Lyman lines of H I, the Lyman and Werner bands of $H_2$ and the atomic fine-structure lines such as C I in the UV as well as a host of rotational lines from molecules in the mm wavelength regime. For example the kinetic temperature of the gas can be determined using either the H I 21 cm line or the $H_2$ UV lines, the pressure and cooling rates can be determined from the fine structure lines of C I and C II* etc. Since many of these tracers co-exist in the diffuse ISM, multi-wavelength observations would allow one to cross check different observational techniques as well as to derive a more complete understanding of the physical state of the ISM.

The gas temperature is a particularly well suited example of a parameter that can, in principle, be determined by observations at a variety of wavelengths. In the radio regime, the classical method consists of observing the H I 21-cm line in absorption towards a bright radio continuum source; this, in conjunction with observations of the emission spectrum along a nearby line of sight allows one to measure the spin temperature ($T_s$) of the H I (see e.g. Kulkarni & Heiles 1988, for details). While the H I spin temperature, strictly speaking, characterizes the population distribution between the two hyperfine levels of the hydrogen atom, it is often used as a proxy for the kinetic temperature of the gas. This is because, in high density regions, $T_s$ is expected to be tightly coupled to the kinetic temperature via collisions, while in low density regions, resonant scattering of Lyman-$\alpha$ photons again may couple the spin temperature to the kinetic temperature (Field 1958). UV observations of the Lyman and Werner bands of $H_2$ also allow one to determine the gas temperature. This is the so called "ortho-para" temperature ($T_{01}$). The ortho-para temperature characterizes the population distribution between the ortho and para forms of the $H_2$ molecule, and like the spin temperature, it too is expected to be coupled to the kinetic temperature of the gas. This happens mainly via proton exchange collisions (e.g. Dalgarno, Black & Weisheit 1973). In regions where H I and $H_2$ co-exist, one might hence expect that the temperatures derived from radio (i.e. $T_s$) and UV observations (i.e. $T_{01}$) should match. However, there have been very limited multi-wavelength studies of this sort. The main reason for this is probably that a given line of sight is rarely suitable for observations at more than one wavelength. For example, UV observations are generally made toward bright nearby stars

⋆ E-mail: nirupam@ncra.tifr.res.in (NR); chengalu@ncra.tifr.res.in (JNC); anand@iucaa.ernet.in (RS)

which have no detectable radio emission. This rules out complimentary 21-cm studies along these lines of sight. Although a direct comparison of the two temperatures along a given line of sight is difficult it is still possible to compare the average properties of the two temperatures measured from different surveys. For example, using a large sample of UV spectra towards nearby stars, Savage et al. (1977) found the mean value of $T_{01}$ to be $77 \pm 17$ K, which is in good agreement with the mean value of the 21-cm $T_s$ in CNM. This lends support to the argument that both these temperatures trace the kinetic temperature of the gas.

The recent large scale high sensitivity and high angular resolution radio surveys like the NRAO VLA Sky Survey (NVSS, Condon et al. 1998) however do allow a way around the problem of finding lines of sight suitable for both UV and radio observations by identifying radio sources that happen to be close to the line of sight to UV bright stars. These radio sources are generally too faint for the classical single dish emission absorption studies, but are well suited for interferometers where the subtraction of the smooth background emission is automatically achieved. In this work we present the results of the Giant Metrewave Radio Telescope (GMRT, Swarup et al. 1991) 21-cm H I observations toward 18 radio sources.

## 2 OBSERVATION AND DATA ANALYSIS

Our sample (drawn from the NVSS catalog), consists of 18 radio sources brighter than 100 mJy. For each source, we require that there should be a star within $30'$, along the line of sight to which $T_{01}$ is available in Savage et al. (1977). Our 18 radio sources correspond to 16 distinct stars, two stars having two corresponding radio sources. The details are summarized in Table 1. The columns in Table 1 are: (1) the name of the optical source and (2) the radio source, (3) the distances to the star, (4) the stellar co-ordinates, (5) the co-ordinates of the corresponding radio source, (6) the total $H_2$ column density from Savage et al. (1977), (7) the line of sight extinction, $E(B-V)$ from Savage et al. (1977), (8) the ortho-para temperature and its error bars (from Savage et al. 1977, as well as from our recalculations from their data, see below), (9) the H I 21-cm spin temperature (see section 3 for details) and (10) the fractional difference between $T_{01}$ and $T_s$. It is clear from Table 1 that lines of sight in our sample span wide range of $E(B-V)$ and $N(H_2)$. The transverse separations of the lines of sight of corresponding UV and radio observations at the distance of the stars ranges from 0.1 to 12.0 pc.

For the 6 sight lines with $N(H_2) \leqslant 10^{17}$ cm$^{-2}$, no error bars for the column densities were available in Savage et al. (1977). For these cases, we obtained the column densities of $H_2$ in J=0, and J=1 rotational levels of ground vibrational level using Voigt profile fitted to the *Copernicus* archival data. Our estimated column densities agree well with that reported by Savage et al. (1977) and we use our computed errors as indicative values while calculating the excitation temperatures for these systems.

The GMRT radio observations were conducted between July 07–10 2002. For all sources the observing frequency was 1419.4 MHz and the total bandwidth was 2 MHz with 128 spectral channels (i.e. a velocity resolution of $\sim 3.3$ km s$^{-1}$). The total on-source time was 3–4 hour on each source. Scans on standard calibrators were used for flux calibration, phase calibration and also to determine the bandpass shape. Data analysis was done using AIPS. After flagging out bad data, the flux density scale and instrumental phase were calibrated. The continuum emission was then subtracted from the multi-channel visibility data set using the task UVSUB. Any residual continuum was then subtracted in the image plane by fitting a linear baseline to line-free regions using IMLIN.

For the 21-cm emission spectra we took data from the Leiden-Dwingeloo survey (Hartmann & Burton 1997). The angular resolution of this survey is $\sim 36'$, i.e. larger than the separation between our target star and the corresponding radio source. The spectral resolution of the raw data is 1.030 km s$^{-1}$, however we Hanning smoothed these spectra to match the resolution of absorption spectra.

## 3 CALCULATIONS

### 3.1 Calculation of spin temperature:

For a homogeneous cloud, the emission and absorption spectra uniquely yield the spin temperature, i.e.

$$T_s = \frac{N(HI)}{1.823 \times 10^{18} \int \tau(v) dv} \quad (1)$$

with N(H I) being determined from the (off source) emission spectrum and $\tau$(v) being determined from the absorption spectrum. In the real life situation where the gas is not homogeneous, but instead has density and temperature structure both along as well as transverse to the line of sight, the determination of "the" spin temperature from radio observations is non trivial. As an example, application of Eq.(1) to the observed spectrum produced by a set of optically thin multiple components along the line of sight will yield a column density weighted harmonic mean temperature of the individual components. If the optical depths are large or there is structure both along and transverse to the line of sight, then in general there is no unique interpretation of the data, although, several approaches to modeling have been attempted (e.g. Mebold 1972; Mebold et al. 1982; Heiles & Troland 2003a,b). We note that though there is no mathematically unique and physically robust procedure to interpret the spectra in this case, much of what we have learned about the neutral atomic medium has comes from the relatively simplistic assumptions underlying Eq. (1). In the analysis presented below, we continue in this tradition.

There is in general absorption at several discrete velocity ranges arising from gas between us and the target star. As the absorption lines of $H_2$ in J=0 and J=1 levels are saturated, it is not possible to obtain the velocity information required to measure $T_{01}$ for individual components; instead what is measured is the line of sight average value of $T_{01}$. It would hence be appropriate to also deal with the average $T_s$. Accordingly, we first independently decomposed the emission and absorption spectra into multiple Gaussian components for the complete available velocity range using least-square minimization with minimum number of components. There is of course some measure of subjectivity in this decomposition. As a check on this,

**Table 1.** Details of our sample and results

| Star HD | Radio Source NVSS | d[a] (pc) | Optical (l, b) (°) | Radio (l, b) (°) | $\log(N_{H_2})^a$ $cm^{-2}$ | E(B-V)[a] mag | $T_{01}$[a] K | $T_s$ K | $\Delta$ T/T |
|---|---|---|---|---|---|---|---|---|---|
| 22928 | J034227+474944 | 82 | 150.28, −05.77 | 150.20, −05.78 | 19.30 | 0.01 | 92 ± 32 | 98 ± 13 | −0.07 ± 0.38 |
| | J034629+474637 | | | 150.76, −05.41 | | | | 119 ± 04 | −0.25 ± 0.35 |
| 22951 | J034300+340634 | 406 | 158.92, −16.70 | 158.93, −16.51 | 20.46 | 0.24 | 63 ± 14 | 77 ± 02 | −0.20 ± 0.22 |
| 23408 | J034440+243622 | 78 | 166.17, −23.51 | 165.78, −23.51 | 19.75 | 0.00 | 89 ± 40 | 103 ± 09 | −0.14 ± 0.45 |
| 36486 | J053413−004408 | 384 | 203.86, −17.74 | 204.54, −17.46 | 14.68 | 0.07 | 1625±863[b] | 219 ± 41 | +1.52 ± 0.23 |
| 36861 | J053450+100430 | 532 | 195.05, −12.00 | 194.89, −11.98 | 19.11 | 0.12 | 45 ± 08 | 92 ± 03 | −0.68 ± 0.15 |
| 37128 | J053550−012448 | 409 | 205.21, −17.24 | 205.36, −17.42 | 16.57 | 0.08 | 108 ± 10[b] | 108 ± 05 | −0.00 ± 0.10 |
| 38771 | J054409−091739 | 520 | 214.51, −18.50 | 213.75, −19.14 | 15.68 | 0.07 | 156 ± 21[b] | 72 ± 01 | +0.74 ± 0.12 |
| 40111 | J055703+261119 | 1247 | 183.97, +00.84 | 183.66, +00.77 | 19.74 | 0.15 | 117 ± 52 | 88 ± 03 | +0.28 ± 0.44 |
| 47839 | J064145+094704 | 705 | 202.94, +02.20 | 203.12, +02.32 | 15.55 | 0.07 | 1153±493[b] | 54 ± 02 | +1.82 ± 0.07 |
| 57060 | J071741−241542 | 1871 | 237.82, −05.37 | 237.46, −05.43 | 15.78 | 0.18 | 82 ± 06[b] | 72 ± 07 | +0.12 ± 0.13 |
| 57061 | J071717−250453 | 933 | 238.18, −05.54 | 238.14, −05.89 | 15.47 | 0.15 | 513 ± 46[b] | 147 ± 03 | +1.11 ± 0.06 |
| 143275 | J160052−221214 | 155 | 350.10, +22.49 | 350.51, +22.70 | 19.41 | 0.16 | 56 ± 12 | 56 ± 01 | +0.00 ± 0.22 |
| | J160401−222341 | | | 350.92, +22.04 | | | | 48 ± 00 | +0.15 ± 0.21 |
| 147165 | J162400−261231 | 142 | 351.31, +17.00 | 351.28, +16.11 | 19.79 | 0.38 | 64 ± 12 | 53 ± 03 | +0.18 ± 0.19 |
| 149757 | J163631−105841 | 138 | 006.28, +23.59 | 005.82, +23.47 | 20.65 | 0.32 | 54 ± 04 | 80 ± 07 | −0.39 ± 0.12 |
| 209975 | J220320+624033 | 1086 | 104.87, +05.39 | 104.94, +05.83 | 20.08 | 0.38 | 77 ± 21 | 67 ± 00 | +0.14 ± 0.26 |
| 224572 | J000020+553908 | 377 | 115.55, −06.36 | 115.72, −06.50 | 20.23 | 0.17 | 82 ± 23 | 191 ± 05 | −0.80 ± 0.24 |

[a] Savage et al. (1977); [b] Error in $T_{01}$ from our calculations

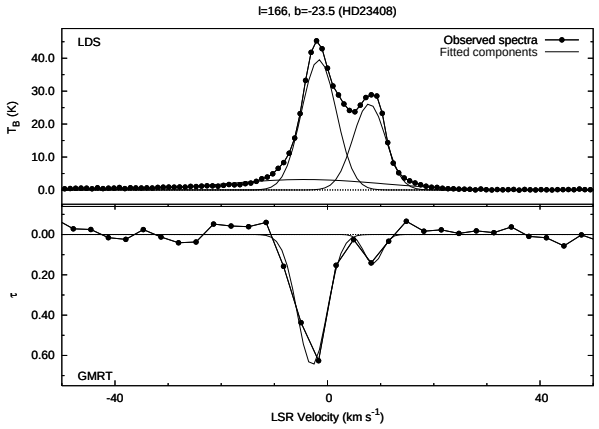


**Figure 1.** Profiles of the observed H I 21-cm emission and absorption towards l=166°, b=−23°.5 (corresponding to J034440+243622). The top panel is the emission spectrum taken from Leiden-Dwingeloo Survey (LDS). The bottom panel is the absorption spectrum taken using GMRT. Note that the broad component in emission is not detected in absorption.

we note that although the decomposition was done independently for the emission and absorption spectra, for most cases we found components whose velocities match within the velocity resolution in the emission and absorption spectra. In some cases there is one or more wide components in the emission spectra which have no corresponding component in the absorption spectra (see Fig. 1). The traditional interpretation of this is that they arise from gas with too high a spin temperature to produce measurable absorption (Radhakrishnan et al. 1972; Heiles 2001; Heiles & Troland 2003a,b), i.e. the warm neutral medium (WNM), although of course it could also arise from a multiple weak narrow components or problems with the spectral baseline. Given the lack of velocity information in the $H_2$ spectra, there is no unique way to match the H I absorption components found in this way with the $H_2$ absorbing gas. We have instead used the velocities of Na I, K I or C I absorption lines (taken from (Jenkins, Jura & Loewenstein 1983; Price et al. 2001; Welty, Hobbs & Kulkarni 1994; Welty & Hobbs 2001; White et al. 2001)) towards these same stars as a guide in this matching process. As the ionization potential of these species are less than that of H I and close to the energy required to destroy $H_2$, they are expected to coexist with $H_2$ in diffuse ISM. One should note however that (i) the combination of galactic rotation and velocity dispersion could cause distant H I to appear at the same velocity as nearby gas, (ii) there could be regions where these ions do not coexist (i.e. the species are in a higher ionization state) but hydrogen is still in neutral state. Both of these mean that one cannot make a robust match between the H I and $H_2$ absorbing gas. We do find however that in most of the cases we can find matching components, and that these components by and large have $|V_{\rm LSR}| \lesssim 10$ km s$^{-1}$ (Given that the stars are relatively nearby $|V_{\rm LSR}| \lesssim 10$ km s$^{-1}$ is a plausible cutoff velocity for gas lying between us and the stars). We therefore proceed by assuming that this matching is statistically correct. The average $T_s$ was then calculated from the integrated emission and absorption spectra for all the matching CNM components. The calculation is done assuming that one is working in the limit of small optical depth, and also with no correction for absorption of the emission from one cloud by another cloud that happens to lie in front of it. This is for two reasons (i) as discussed above, there is no unique way to make this correction and (ii) as discussed in more detail below, we expect all such corrections to lie within the error bars of the $T_{01}$ measurement. The errors in $T_s$ were estimated from the rms noise of the spectra and the FWHM of the Gaussian component for emission and absorption. This error should be taken only as an indicative value as it does not account for the error in fit and the error introduced through the assumption of small $\tau$. However, since the error

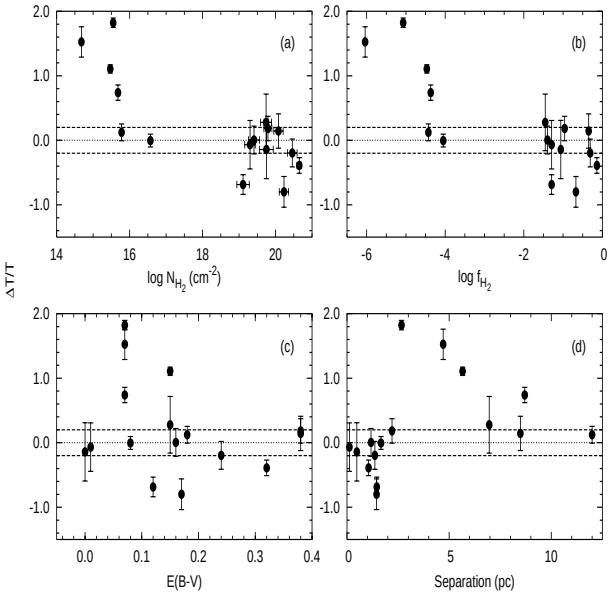


**Figure 2.** $\Delta$T/T as a function of different physical quantities. The horizontal lines in the figures mark $\Delta$T/T = 0 and 20% uncertainty.

bars are in general small compared to the error bars in $T_{01}$, the indicative value should suffice.

### 3.2 Calculation of ortho-para temperature:

It is a standard procedure, in ISM studies, to use measured ortho-to-para ratio (OPR) of $H_2$ to infer the kinetic temperature of the gas. If we assume most of the ortho and para $H_2$ reside in their respective ground levels then we can write,

$$\mathrm{OPR} \simeq \frac{\mathrm{N(J=1)}}{\mathrm{N(J=0)}} = 9\ \exp(-170.5/\mathrm{T_{01}})\ . \qquad (2)$$

$T_{01}$ derived from the above equation will either trace the kinetic temperature of the gas (if OPR is controlled by proton or hydrogen exchange collisions) or formation temperature (if OPR is controlled by reactions in the grain surface) of $H_2$ (for details refer to Sternberg & Neufeld 1999; Takahasi 2001). We have used the observed column densities given in Table 1 and Eq.(2) to estimate $T_{01}$. The associated error is computed using the standard error propagation. Since we can not resolve individual components, the derived $T_{01}$ is the average temperature along the line of sight.

## 4 RESULTS

We define, the fractional difference between $T_s$ and $T_{01}$ by

$$\Delta\mathrm{T/T} = \frac{2(\mathrm{T_{01}} - \mathrm{T_s})}{(\mathrm{T_{01}} + \mathrm{T_s})} \qquad (3)$$

From Table 1 we can see that $\Delta$T/T = 0 within measurement uncertainties for nine out of 16 cases. For three sightlines we find $T_s > T_{01}$ and the other four sightlines have $T_s < T_{01}$. From the Fig. 2 it is also clear that the points with $\Delta$T/T $\simeq$ 0 spread over the whole range of $E(B-V)$ and line of sight separation covered in our sample. However, the points with $\Delta$T/T > 0 mainly come from the sightlines that have log N($H_2$)$\leqslant$ 15.8 or molecular fraction $f_{H_2}$(=2N($H_2$)/2N($H_2$)+N(H I)) $\leqslant 10^{-4}$. This is expected as Solomon pumping dominates the excitation in this regime. The three points with $\Delta$T/T < 0 are from lines of sight that are optically thick in $H_2$ with $f_{H_2} \geqslant 10^{-2}$ and may be region where H I and $H_2$ are not co-existing. In panel (d) we plot $\Delta$T/T as a function of maximum separation between optical and radio sightlines. We do not find any clear trend in this plot. We explore this issue further by collating in Table 2 the cases where we have more than 1 radio source or star within a separation of 1°. The columns in the table are (1) the name of the sources, (2) position, (3) separation of the lines of sight (ds) at the distance of the star, (4) N(H I) and (5) the temperature ($T_{01}$ or $T_s$) measured along the line of sight. We find, among the cases where $T_{01} \simeq T_s$, the match generally improves with decreasing separation, though there are cases (e.g. HD36861) where the temperatures do not match even for a separation of 1.45 pc. One should note however that the separations are computed assuming the gas is at the distance of the star, while in reality the gas could lie anywhere between us and the star.

**Table 2.** Spatial variation of temperature:

| Source HD | Position l (°) | b (°) | ds [pc] | logN(HI) (cm$^{-2}$) | T [K] |
|---|---|---|---|---|---|
| HD22928 | 150.28 | −05.77 | — | — | 92 |
| radio1 | 150.20 | −05.78 | 0.12 | 20.87 | 98 |
| radio2 | 150.76 | −05.41 | 0.86 | 21.14 | 119 |
| HD23408 | 166.17 | −23.51 | — | — | 89 |
| radio1 | 165.78 | −23.51 | 0.48 | 21.00 | 103 |
| HD23480 | 166.57 | −23.75 | 0.60 | — | 67 |
| HD36861 | 195.05 | −12.00 | — | 20.78 | 45 |
| radio1 | 194.89 | −11.98 | 1.45 | 20.68 | 92 |
| HD36822 | 195.40 | −12.29 | 4.16 | 20.81 | 63 |
| HD37128 | 205.21 | −17.24 | — | 20.45 | 108 |
| radio1 | 205.36 | −17.42 | 1.67 | 20.92 | 108 |
| HD37742 | 206.45 | −16.59 | 9.65 | 20.41 | 101 |
| HD57060 | 237.82 | −05.37 | — | 20.70 | 82 |
| radio1 | 237.46 | −05.43 | 12.00 | 20.51 | 72 |
| HD57061 | 238.18 | −05.54 | 12.95 | 20.70 | 513 |
| radio2 | 238.14 | −05.89 | 19.89 | 20.24 | 147 |
| HD143275 | 350.10 | +22.49 | — | 21.15 | 56 |
| radio1 | 350.51 | +22.70 | 1.17 | 21.09 | 56 |
| radio2 | 350.92 | +22.04 | 2.38 | 20.60 | 48 |

## 5 DISCUSSION

In this work we present the GMRT measurement of 21-cm spin temperature toward 18 radio sources that are close to 16 bright starts for which UV observations are available. We find the $T_s$ and $T_{01}$ trace each other within the observational uncertainties when N($H_2$)$\geqslant 10^{15.8}$ cm$^{-2}$ in 75 per cent of the cases. $T_{01}$ is found to be higher than $T_s$ for the sightlines with low $H_2$ column density.

Heiles & Troland (2003a) have performed similar analysis like us towards three directions. There is one star in our sample (HD 22951) that is in common with Heiles & Troland (2003a). For this sightline $T_{01}$ = 63±14 K and we find consistent $T_s$ = 77±2 toward a radio source with a maximum separation of 1.35 pc. Heiles & Troland (2003a) report $T_{01}$ = 27±13 and 29±11 K toward NRAO 140 and 3C93.1 that are separated by 14.6 and 9.5 pc respectively from the star. The spin temperature that they quote is that for a single CNM component along the line of sight. If we instead use the column density weighted average of all CNM components in the velocity range probed by the C I absorption (Jenkins et al. 1983), the spin temperatures are 53 and 72 K, i.e. in agreement with $T_{01}$.

A major concern is that we do not know if our temperature comparisons are for the same gas; we have only a plausible matching between the H I and $H_2$ absorbing gas. As discussed above though, this matching is likely to be on the average correct. If this is so, then our findings mean that $T_s$ and $T_{01}$ do not vary much over distances of a few parsecs. This is in apparent contrast to the well known findings that the H I 21-cm opacity varies on much smaller spatial scales (e.g. Dieter, Welch & Romney 1976; Crovisier, Dickey & Kazès 1985). The resolution may be that the opacity fluctuations reflect not so much fine scale structure in the temperature as fine scale structure in the velocity and density fields (e.g. Brogan et al. 2005). It is also possible that our averaging over the several line of sight components decreases the effects of small scale variations.

Another issue is related to the relatively large error bars in $T_{01}$. Is it possible that all that our data is telling us is that the CNM has a characteristic temperature $\sim$ 80 K, and that the general agreement between $T_{01}$ and $T_s$ merely reflects the fact that both the UV and radio observations are probing the CNM? Or does the temperature agreement actually extend to individual lines of sight, as we have been asserting? A least-square linear fit using all 11 lines of sight for which $T_{01}$ and $T_s$ agree (including both the radio sources close to HD22928 and HD143275) for $T_{01} = r\,T_s$ gives r= 0.981 ± 0.054. For all the lines of sight with $H_2$ column density higher than our threshold, the least-square fit gives r= 0.778±0.080. As a quantitative check, we have calculated the Spearman correlation coefficient for increasingly larger subsamples. For a subsample with all 11 lines of sight for which $T_s$ matches $T_{01}$, the correlation coefficient is maximum (0.648). The corresponding significance is $p < 0.05$ (from a two-tailed test). For a subsample with all 14 lines of sight for which $H_2$ column density is more than $10^{15.8}$ $cm^{-2}$, the correlation coefficient is 0.545. On the other hand when one includes lines of sight with $N(H_2)$ less than $10^{16}$ $cm^{-2}$, the correlation coefficient goes down to 0.406 (for our complete sample). To summarize then, as per the Spearman rank coefficient test, at the better than 95% level, there is a one to one relation between $T_{01}$ and $T_s$ for the 11 lines of sight with $N(H_2)$ higher than $10^{15.8}$ $cm^{-2}$. Agreement between $T_s$ and $T_{01}$ for high column density gas would mean that the ortho-para equilibrium is mainly due to exchange collisions and that $T_{01}$ does not reflect the formation temperature. The absence of relation between the two temperatures when $N(H_2)$ is optically thin is consistent with the slow rate of exchange collisions compared to the $H_2$ destruction rate and excess Solomon pumping from J=0 and J=1 levels that make $T_{01}$ deviate from the kinetic temperature and hence $T_s$.

## ACKNOWLEDGMENTS

The observations presented in this paper were obtained using the GMRT which is operated by the National Centre for Radio Astrophysics (NCRA) of the Tata Institute of Fundamental Research (TIFR), India. We are grateful to the anonymous referee for prompting us into substantially improving this paper. Some of the data presented in this paper were obtained from the Multimission Archive at the Space Telescope Science Institute (MAST).

## REFERENCES

Brogan C. L., Zauderer B. A., Lazio T. J., Goss W. M., De Pree C. D. & Fasion M. D. 2005, AJ (accepted, astro-ph/0505080)
Condon J. J., Cotton W. D., Greisen E. W., Yin Q. F., Perley R. A., Taylor G. B., Broderick J. J., 1998, AJ, 115, 1693
Crovisier J., Dickey J. M., Kazès I., 1985, A&A, 146, 223
Dalgarno A., Black J. H., Weisheit J. C., 1973, ApL., 14, 77
Dieter N. H., Welch W. J., Romney J. D., 1976, ApJ, 206, L113
Field G. B., 1958, Proc. IRE, 46, 240
Hartmann D., Burton W. B., 1997, Atlas of Galactic Neutral Hydrogen, Cambridge University Press, Cambridge, NY
Heiles C., 2001, ApJ, 551, L105
Heiles C., Troland T. H., 2003a, ApJ, 586, 1067
Heiles C., Troland T. H., 2003b, ApJS, 145, 329
Jenkins E. B., Jura M., Loewenstein M., 1983, ApJ, 270, 88
Kulkarni S. R., Heiles C., 1988, Neutral hydrogen and the diffuse interstellar medium, in Galactic and extragalactic radio astronomy (2nd ed.; Springer-Verlag), 95
Mebold U., 1972, A&A, 19, 13
Mebold U., Winnberg A., Kalberia P. M. W., Goss W. M., 1982, A&A, 115, 223
Price R. J., Crawford I. A., Barlow M. J., Howarth I. D., 2001, MNRAS, 328, 555
Radhakrishnan V., Murray J. D., Lockhart Peggy, Whittle R. P. J., 1972, ApJS, 24, 15
Savage B. D., Drake J. F., Budich W., Bohlin R. C., 1977, ApJ, 216, 291
Sternberg A., Neufeld D. A., 1999, ApJ, 516, 371
Swarup G., Ananthakrishnan S., Kapahi V. K., Rao A. P., Subrahmanya C. R., Kulkarni V. K., 1991, Curr. Sci., 60, 95
Takahasi J., 2001, ApJ, 561, 254
Welty D. E., Hobbs L. M., Kulkarni V. P., 1994, ApJ, 436, 152
Welty D. E., Hobbs L. M., 2001, ApJS, 133, 345
White R. E., Allen C. L., Forrester W. B., Gonnella A. M., Young K. L., 2001, ApJS, 132, 253

This paper has been typeset from a TEX/ LATEX file prepared by the author.